Structural Damage Identification Based on Substructure Sensitivity and l_1 Sparse Regularization

Yuequan BAO[*], Shumei ZHOU[*], Hui LI[*], Jinping OU[*, **]
[*]School of Civil Engineering, Harbin Institute of Technology, Harbin, 150090, China
[**]School of Civil and Hydraulic Engineering, Dalian University of Technology, Dalian, 116024, China

Abstract. Sparsity constraints are now very popular to regularize inverse problems in the field of applied mathematics. Structural damage identification is a typical inverse problem of structural dynamics and Structural damage is a spatial sparse phenomenon, i.e., structural damage occurs, only part of elements or substructures are damaged. In this paper, a structural damage identification method based on the substructure-based sensitivity analysis and the sparse constraints regularization is proposed. Substructure sensitivity analysis, the establishment of structural damage stiffness parameter variation and change of modal parameters of linear equations between the measured degrees of freedom is limited, the equations for a morbid equation. The introduction of structural damage sparsity conditions, to minimize the *l*1 norm optimization solution. The numerical example of the 20 bay-truss structure with considering measurement noise, incomplete of measurements and multi-damage cases are carried out. The effects of number sensor and layout to the identification results are also investigated. The results indicated that the damage locations and extents can be effectively identified by the proposed method. Additionally, the sensor location can be random arrangement, which has great significance to the sensor placement of the actual structural health monitoring because robust structural damage identification also can be obtained even a few of sensor are failure.

1 Introduction

Structural damage detection is a core issue of structural health monitoring, which has been investigated long times and a lot of methods has been proposed [1].These methods can be divided in accordance with the need for the point of view of the finite element model, model and non-model-based damage identification methods.

The non-model based damage identification method firstly identify the modal parameters or directly extract damage features from the response data, and then construct the sensitive damage indexes for identify the damage of structure. Such as frequency-based methods which construct the suitable indicator for damage identification through structural frequency change. The mode shapes based methods detect the damage by the changes of mode shapes before and after structural damage, which including the MAC, mode curvature, stiffness method and flexibility, residual force, modal strain energy methods. The others methods including wavelet damage feature extraction method [2] or HHT (Hilbert Huang Translation) method [3] are all the non-model based damage identification methods.

The finite element (FE) model has an important role in the damage identification of structure. The model based methods used the modal parameters or damage characteristic

License: http://creativecommons.org/licenses/by/3.0/

parameters extracted from structural vibration response data combing with the FE model to identify the structure parameters, and then proceed to the damage identification, such as the Bayesian damage detection methods [4]. For these methods, the most important is identification of system parameters by optimization problems. Recently, sparsity constraints are now very popular to regularize inverse problems in the field of applied mathematics. For example, the compressive sensing (CS) technique [5-8], which the core idea is a high-dimensional signal is compressible or sparsity in a transform domain, then you can use a transform base irrelevant projected onto a low dimensional space of the signal of the measurement matrix, and then by solving an optimization problem to reconstruct the original signal from the small amount of projection with overwhelm probability. Essentially, the CS is to find the sparse solutions of underdetermined equation. The investigation of CS theory also put forward the development of sparse regularization of inverse problem, which provide a new way for the solving of inverse problem which has sparsity in time domain, spatial domain or some base transformation. Structural damage identification is a typical inverse problem of structural dynamics and Structural damage is a spatial sparse phenomenon. In this paper, a structural damage identification method based on the substructure-based sensitivity analysis and the sparse constraints regularization is proposed.

2 Substructure Sensitivity coefficients analysis

Sensitivity coefficients analysis for vibration parameters is a mature technique. Stiffness, mass and damping changes often result in changes in different diagnostic parameters, including natural frequencies and mode shapes. The changes in stiffness coefficients for a FE model are used to represent damage in this study, and the first order sensitivity coefficients for the natural frequencies and the mode shapes to the damage of substructure are derived.

For a structural system with N degrees of freedom, the natural frequencies, $\omega_r \ \left(r=1,2,...,N\right)$ and mode shapes, $\boldsymbol{\varphi}_r \left(r=1,2,...,N\right)$, can be determined with a FE analysis. The equilibrium equation for undamped structural vibration equation is

$$\left(\mathbf{K}-\omega_r^2\mathbf{M}\right)\boldsymbol{\varphi}_r=0 \tag{1}$$

where $\mathbf{M}$ and $\mathbf{K}$ are mass and stiffness matrices; ω_r and $\boldsymbol{\varphi}_r$ are rth ($r=1,2,\cdots,N$) frequency and mode shape, where $\boldsymbol{\varphi}_r$ is the normalized to be unit-mass mode shapes, i.e. $\boldsymbol{\varphi}_r^T\mathbf{M}\boldsymbol{\varphi}_r=1$.

The stiffness matrix can be represent as,

$$\mathbf{K}=\sum_{i=1}^{N_\theta}\left(1-\theta_i\right)\mathbf{K}_i \tag{2}$$

where $\mathbf{K}_i$ is the substructure stiffness contribution to the global stiffness matrix which could come from a FE model of undamaged structure; $\theta_i \ \left(i=1,2,...,N_\theta\right)$ is stiffness damage parameter and N_θ is the number of substructure.

2.1 Sensitivity coefficients for natural frequency

The first order sensitivity coefficients for natural frequency with respect to the parameter θ_i can be calculated by derivative of Eq. (1) with respect to θ_i as

$$\left(\frac{\partial\mathbf{K}}{\partial\theta_i}-2\omega_r\frac{\partial\omega_r}{\partial\theta_i}\mathbf{M}-\omega_r^2\frac{\partial\mathbf{M}}{\partial\theta_i}\right)\boldsymbol{\varphi}_r+\left(\mathbf{K}-\omega_r^2\mathbf{M}\right)\frac{\partial\boldsymbol{\varphi}_r}{\partial\theta_i}=0 \tag{3}$$

Both sides of this equation are premultiplied by $\boldsymbol{\varphi}_r^T$. By utilizing the known relations including $\boldsymbol{\varphi}_r^T \mathbf{M} \boldsymbol{\varphi}_r = \mathbf{I}$ for the unit-mass mode shapes, Eq. (1) and that $\mathbf{M}$ is independent of θ_i (therefore $\partial \mathbf{M} / \partial \theta_i = 0$), it can be shown that sensitivity coefficient of the *r*th natural frequency in terms of θ_i can be derived as

$$\frac{\partial \omega_r}{\partial \theta_i} = \frac{1}{2\omega_r} \boldsymbol{\varphi}_r^T \frac{\partial \mathbf{K}}{\partial \theta_i} \boldsymbol{\varphi}_r \tag{4}$$

Note that $\mathbf{K} = \sum_{i=1}^{N_\theta} (1 - \theta_i) \mathbf{K}_i$

$$\frac{\partial \mathbf{K}}{\partial \theta_i} = \partial \left(\sum_{i=1}^{N_\theta} (1 - \theta_i) \mathbf{K}_i \right) \Big/ \partial \theta_i = -\mathbf{K}_i \tag{5}$$

Thus, the sensitivity coefficients of the natural frequencies can be rewritten as

$$\mathbf{S}_\omega = \frac{\partial \omega_r}{\partial \theta_i} = -\frac{1}{2\omega_r} \boldsymbol{\varphi}_r^T \mathbf{K}_i \boldsymbol{\varphi}_r \tag{6}$$

2.2 Sensitivity coefficients for mode shapes

The derivation of first order sensitivity coefficients for mode shapes can refer the paper of Zhao and DeWolf [9]. In the paper, the derivation of mode shapes is respect to stiffness damage parameter θ_i. As represented in Zhao and DeWolf [9], the sensitivity coefficients of *r*th mode shape can be defined as follows:

$$\mathbf{S}_\varphi = \frac{\partial \boldsymbol{\varphi}_r}{\partial \theta_i} = \sum_{l=1}^{N} \alpha_l \boldsymbol{\varphi}_l \tag{7}$$

where α_L is undetermined coefficient that represents weight of the lth mode shape in the sensitivity coefficient. Two possibilities exist for α_l:

(1) When $s \neq r$, where s is subscript of the coefficient of α, α_s are the weights of all mode shapes except the rth mode shape used for the right side of Eq. (7). Eq. (3) is premultiplied by $\boldsymbol{\varphi}_s^T$ on both sides. Since mode shapes are orthogonal, it can be shown that $\boldsymbol{\varphi}_s^T \mathbf{M} \boldsymbol{\varphi}_r = 0$, if $s \neq r$; $\boldsymbol{\varphi}_s^T \mathbf{M} \boldsymbol{\varphi}_s = \mathbf{I}$; $\boldsymbol{\varphi}_s^T \mathbf{K} = \omega_s^2 \boldsymbol{\varphi}_s^T \mathbf{M}$; and $\partial \mathbf{M} / \partial \theta_i = 0$.

Eq. (1) can be then be written as

$$-\boldsymbol{\varphi}_s^T \mathbf{K}_i \boldsymbol{\varphi}_r - \boldsymbol{\varphi}_s^T \left(\omega_r^2 - \omega_s^2 \right) \mathbf{M} \sum_{l=1}^{n} \alpha_l \boldsymbol{\varphi}_l = \mathbf{0} \tag{8}$$

For unit-mass normalized mode shapes, Eq. (13) can be rewritten as

$$\alpha_s \left(\omega_s^2 - \omega_r^2 \right) = \boldsymbol{\varphi}_s^T \mathbf{K}_i \boldsymbol{\varphi}_r \tag{9}$$

Solving for α_s

$$\alpha_s = \frac{1}{\left(\omega_s^2 - \omega_r^2 \right)} \boldsymbol{\varphi}_s^T \mathbf{K}_i \boldsymbol{\varphi}_r \tag{10}$$

(2) When $s = r$, α_s is the weights of the *r*th mode shape used for the right side of (2). For the unit-mass normalized mode shapes it is

$$\boldsymbol{\varphi}_r^T \mathbf{M} \boldsymbol{\varphi}_r = \mathbf{I} \tag{11}$$

Taking derivative of Eq. (11) with respect to θ_i results in

$$\frac{\partial \boldsymbol{\varphi}_r^T}{\partial \theta_i}\mathbf{M}\boldsymbol{\varphi}_r + \boldsymbol{\varphi}_r^T\mathbf{M}\frac{\partial \boldsymbol{\varphi}_r}{\partial \theta_i} = 0 \tag{12}$$

Considering the symmetry property of a mass matrix

$$\frac{\partial \boldsymbol{\varphi}_r^T}{\partial \theta_i}\mathbf{M}\boldsymbol{\varphi}_r = \boldsymbol{\varphi}_r^T\mathbf{M}\frac{\partial \boldsymbol{\varphi}_r}{\partial \theta_i} \tag{13}$$

and using Eq. (7), Eq. (12) can be rewritten as

$$2\sum_{l=1}^{n}\alpha_l\boldsymbol{\varphi}_r^T\mathbf{M}\boldsymbol{\varphi}_l = 0 \tag{14}$$

Based on the orthogonal properties of the mode shapes and Eq. (14), it can be shown that

$$\alpha_r = 0 \tag{15}$$

Thus the sensitivity coefficients for the mode shapes can be summarized as follows:

$$\mathbf{S}_\varphi = \begin{cases} \dfrac{1}{\left(\omega_s^2 - \omega_r^2\right)}\boldsymbol{\varphi}_s^T\mathbf{K}_i\boldsymbol{\varphi}_r & s \neq r \\ 0 & s = r \end{cases} \tag{16}$$

3 Damage identification approach

The structure is assumed to behave linearly before and after the occurrence of damage. The relation between the changes of modal parameters $\Delta\boldsymbol{\gamma} = [\Delta\boldsymbol{\omega}, \Delta\boldsymbol{\varphi}]^T$ and substructure stiffness damage parameters $\boldsymbol{\theta}$ can be expressed as

$$\Delta\boldsymbol{\gamma} = \mathbf{S}\boldsymbol{\theta} \tag{17}$$

where $\boldsymbol{\theta} = \left[\theta_1, \theta_1, \cdots, \theta_{N_\theta}\right]^T$ is stiffness damage parameters vector which represents the damage extent of the substructures; $\mathbf{S}$ is the sensitivity matrix.

$$\mathbf{S} = \left[\mathbf{S}_\omega, \mathbf{S}_\phi\right]^T \tag{18}$$

where $\mathbf{S}_\omega$ and $\mathbf{S}_\phi$ are the sensitivity matrix of the frequency and mode shape, which contains sensitivity coefficients vector of the rth $\left(r = 1, 2, ..., N\right)$ frequency and mode shapes.

$$\mathbf{S}_\omega = \left[\mathbf{S}_{\omega_1}, \mathbf{S}_{\omega_2}, \cdots, \mathbf{S}_{\omega_n}\right]^T,\ \mathbf{S}_\varphi = \left[\mathbf{S}_{\varphi_1}, \mathbf{S}_{\varphi_2}, \cdots, \mathbf{S}_{\varphi_n}\right]^T \tag{19}$$

The changes of modal parameters $\Delta\boldsymbol{\gamma}$ including changes of frequency and mode shapes caused by damage of structures is

$$\Delta\boldsymbol{\gamma} = \left[\Delta\boldsymbol{\omega}, \Delta\boldsymbol{\varphi}\right]^T \tag{20}$$

where $\Delta\boldsymbol{\omega}$ and $\Delta\boldsymbol{\varphi}$ are

$$\Delta\boldsymbol{\omega} = \left[\Delta\omega_1, \Delta\omega_2, \cdots, \Delta\omega_n\right]^T,\quad \Delta\boldsymbol{\varphi} = \left[\Delta\boldsymbol{\varphi}_1, \Delta\boldsymbol{\varphi}_2, \cdots, \Delta\boldsymbol{\varphi}_n\right]^T \tag{21}$$

Supposing only small number of substructures are damaged, therefore, only small number of the elements of vector $\boldsymbol{\theta} = \left[\theta_1, \theta_1, \cdots, \theta_{N_\theta}\right]^T$ are nonzero, which is sparsity. Considering the limitation of sensors and incompletion of measured modal parameters, m number of sensors are used and N_r number of modals are obtained. With considering the unavoidable measurement noise, the Eq. (17) is changed as

$$\Delta\hat{\boldsymbol{\gamma}} = \hat{\mathbf{S}}\boldsymbol{\theta} + \mathbf{e} \tag{22}$$

where $\mathbf{e}$ is the error caused by measurement noise; $\Delta\hat{\boldsymbol{\gamma}}$ is the actual measured changes of modal parameters.

$$\Delta\hat{\boldsymbol{\gamma}} = \left[\Delta\hat{\boldsymbol{\omega}}, \Delta\hat{\boldsymbol{\varphi}}\right]^T \tag{23}$$

where $\Delta\hat{\boldsymbol{\omega}}$ and $\Delta\hat{\boldsymbol{\varphi}}$ are

$$\Delta\hat{\boldsymbol{\omega}} = \left[\hat{\omega}_1, \hat{\omega}_2, \cdots, \hat{\omega}_n\right]^T, \quad \Delta\hat{\boldsymbol{\varphi}} = \left[\boldsymbol{\Gamma}\Delta\boldsymbol{\varphi}_1, \boldsymbol{\Gamma}\Delta\boldsymbol{\varphi}_2, \cdots, \boldsymbol{\Gamma}\Delta\boldsymbol{\varphi}_n\right]^T \tag{24}$$

where the $\boldsymbol{\Gamma} \in \Re^{m\times n}$ is a random sampling operator comprised of zeros and units and maps the rth whole theoretical mode shapes vector $\boldsymbol{\varphi}_r$ to the observed cable forces $\hat{\boldsymbol{\varphi}}_r = \boldsymbol{\Gamma}\boldsymbol{\varphi}_r$. For convenience, introducing a vector $\boldsymbol{\delta} \in R^{n\times 1}$ with elements $\delta_j = 1$ if the jth degree of freedom is observed and $\delta_j = 0$ if the jth degree of freedom is not installed with a sensor, it can be readily known that $\boldsymbol{\Gamma}^T\boldsymbol{\Gamma} = diag\left(\boldsymbol{\delta}\right)$. The randomness of matrix $\boldsymbol{\Gamma}$ means that the selection of test points to be observed is random.

Eq. (21) is ill-conditioned like many inverse problems. Traditionally, least squares method is used to solve this type of problem, and singular value decomposition is used to find the pseudo-inverse. In Eq. (21), the vector $\hat{\boldsymbol{\theta}}$ is known to be sparse. Therefore, according to CS theory, the solution $\hat{\boldsymbol{\theta}}$ can be obtained by solving the following optimization problem.

$$\min\left\|\tilde{\boldsymbol{\theta}}\right\|_1 \text{ 且 } \left\|\hat{\mathbf{S}}\tilde{\boldsymbol{\theta}} - \Delta\hat{\boldsymbol{\gamma}}\right\|_2 \le \varepsilon \tag{25}$$

where ε is an upper bound of the error which satisfies $\left\|e\right\|_2 \le \varepsilon$. This is the l_1 optimization problem, where the l_1-term enforces the sparsity of the representation.

An unconstrained form of this objective is

$$\hat{\boldsymbol{\theta}} = \arg\min\left(\left\|\hat{\mathbf{S}}\tilde{\boldsymbol{\theta}} - \Delta\hat{\boldsymbol{\gamma}}\right\|_2 + \lambda\left\|\tilde{\boldsymbol{\theta}}\right\|_1\right) \tag{26}$$

where λ is the Lagrange multiplier and identified as a regularization parameter. This objective function has been used in a number of sparse signal representation works [10]. The l_2-term makes the residual $\hat{\mathbf{A}}\tilde{\mathbf{p}}\left(k\right) - \hat{\mathbf{f}}\left(k\right)$ small, while the l_1-term enforces the sparsity of the representation. The parameter λ controls the trade-off between the sparsity of the spectrum and residual norm. Eq. (26) is efficiently solvable with the interior point solvers [10] and the convex optimization package CVX (available at http://cvxr.com/cvx) is used. A proper Lagrange multiplier λ is important to obtain meaningful solutions to Eq. (26) and can be calculated by empirical or iterative methods [11-12].

4 Numerical Examples

The 20-bay rigid truss structure for numerical example is shown in Figure 1, of which the total length, width and height are 8.0, 0.8 and 0.56m, respectively. It consists of 312 members with 108 nodes and all the members are steel bars. The connections of the members are bolt-node balls which are the half-rigidity connections. There are two supports at the ends of the structure: a hinge support at the right end and a vertical roller support at the left.

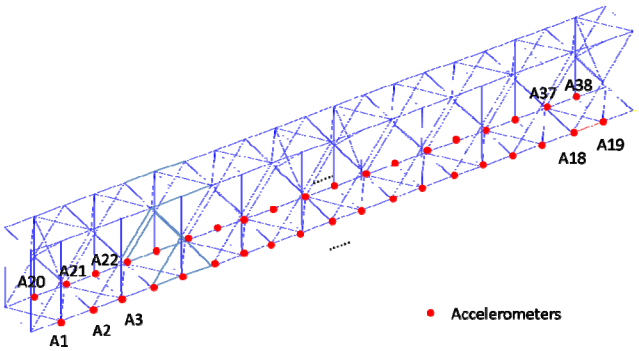

Fig. 1. FE model of 20 bay truss structure

Considering the limited test points in real application, 38 accelerometers are placed on the node of bottom chord of structure as shown in Fig. 1. The damage is simulated by decreasing the Young's modulus of elements. Three damage cases are considered. Damage case 1 is that the element No. 235 damaged 10%. Damage case 2 has two elements of No. 175 and 236 are damaged with 10%, respectively. Damage case 3 has five elements of No. 26, 60, 175, 190 and 265 are damaged with 5%, 5%, 10%, 10% and 10% respectively.

More explicitly, the estimated modal parameter set $\hat{\psi}(n)$ was constructed as:

$$\hat{\psi} = \psi(1 + \varepsilon r) \tag{27}$$

where ψ was the exact modal parameter set obtained from modal analysis, r was a normally distributed random number with zero mean and a variance of 1.0, ε was the noise level in terms of percentage, which the values are 1%, 5% and 10% in this example.

4.1 Damage identification results

Damage identification results of Case 1 are shown in Fig. 2, where Fig. 2(a) is the actual damage and Figs. 2(b-d) are the identified results with considering noise 1%, 5% and 10%, respectively. Fig. 2 shows that the damage location and extent are identified well for Case 1 even with 10% noise.

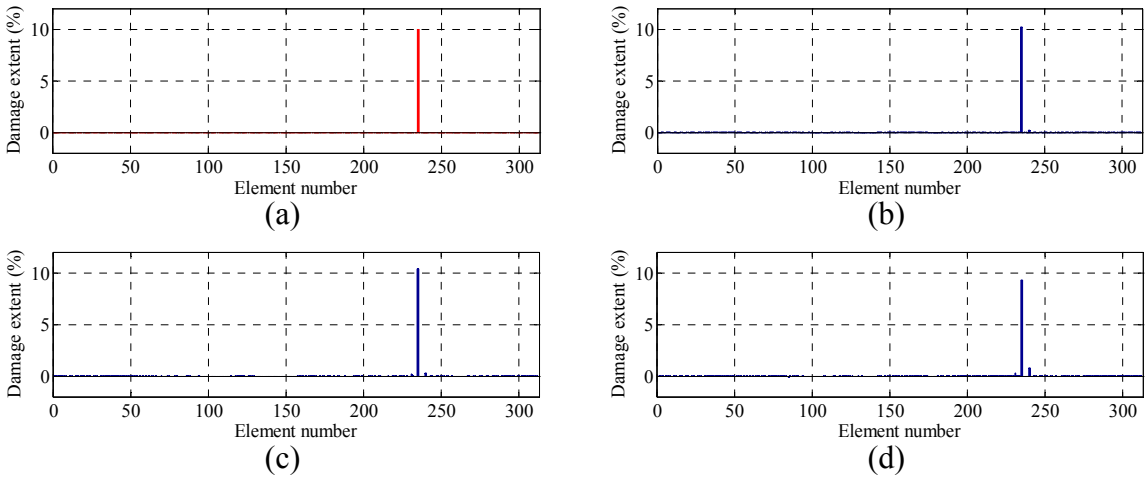

Fig. 2. Damage identification results of Case 1: (a) actual damage; (b) damage identification results with 1% noise; (c) damage identification results with 5% noise; (d) damage identification results with 10% noise;

Damage case 2 has five damaged elements, which the identification results are shown in Fig. 3. Fig. 3(a) is the actual damage of structure which shows the elements no. 26, 60, 175, 190 and 265are damaged 5%, 5%, 10%, 10% and 10%, respectively. Fig. 3(b-d) shows the identification results with 1%, 5% and 10% noise, respectively. Fig. 3 shows that for the multiple damage cases, the proposed approach also can identify the damage

accurately. Comparing with the cases of small amount of elements damaged such as damage case 1 and case 2, the damage cases 3 are more sensitive to the noise as results shown in Fig. 3(d), however, which is also can be acceptable.

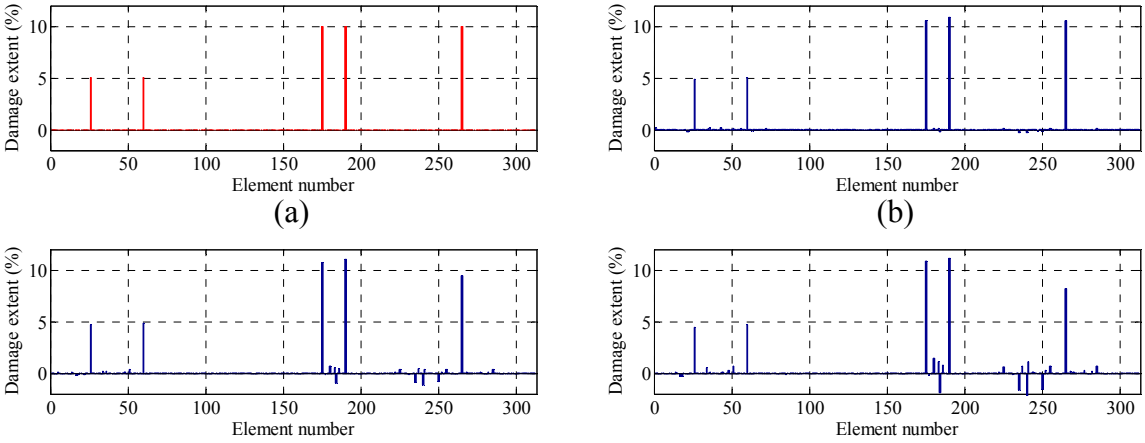

Fig. 3. Damage identification results of Case 3: (a) actual damage; (b) damage identification results with 1% noise; (c) damage identification results with 5% noise; (d) damage identification results with 10% noise;

4.2 Effects of sensor number

To investigate the effects of sensor number on damage identification results, the sensor number from $[8,10,...,38]$ are considered. With difference sensor number, the identification error is calculated by

$$\xi = \left\| \frac{\hat{\boldsymbol{\theta}} - \breve{\boldsymbol{\theta}}}{\breve{\boldsymbol{\theta}}} \right\| \tag{28}$$

where $\hat{\boldsymbol{\theta}}$ is the identified stiffness damage coefficients; $\breve{\boldsymbol{\theta}}$ is the actual stiffness damage coefficients.

The damage identification results are shown in Fig. 4, which shows that with the increasing of sensor number, the damage identification accuracy is increased and this effect is more significant to the multiple damage cases. With same sensor number, the increasing of noise also will increase the damage identification accuracy.

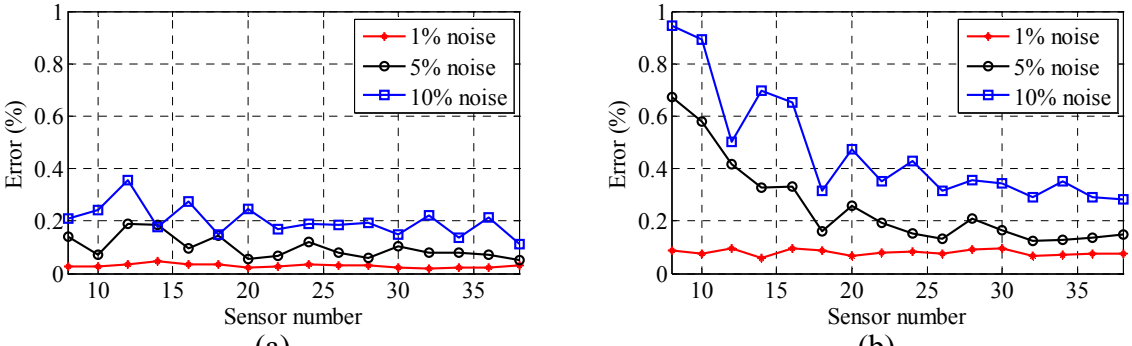

Fig. 4. Relationship between identification error and sensor number: (a) damage case 1; (b) damage case 2

4.3 Effects of sensor location

According to the CS, the selection of location of test points can be random. To show the effects of sensor location, 24 sensors with randomly placed are considered as shown in Fig. 5.

With 24 test points, the damage identification results of the three damage cases with 10% noise are shown in Fig. 6, which shows the damage also can be well identified. This further illustrates the robust results of the proposed approach. Random placement of sensors has remarkable advantages in actual application of SHM systems. Comparing with the traditional senor optimal placement algorithms, randomly placed is much more easily and convenient implement. Otherwise, in actual SHM systems, the complex service environment will cause the failure of sensors and this phenomenon is random. If one or small number of sensors are failed, the robust damage identification results also can be obtained.

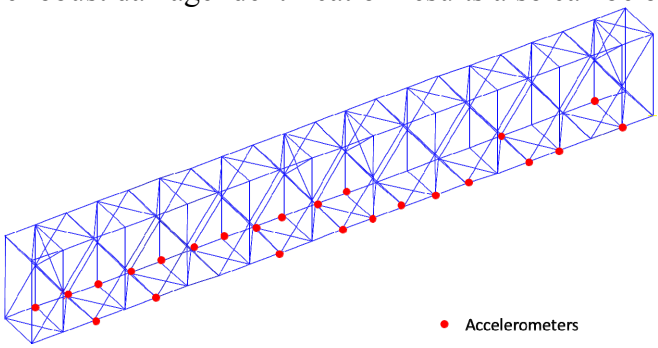

Fig. 5 Locations of 24 test points

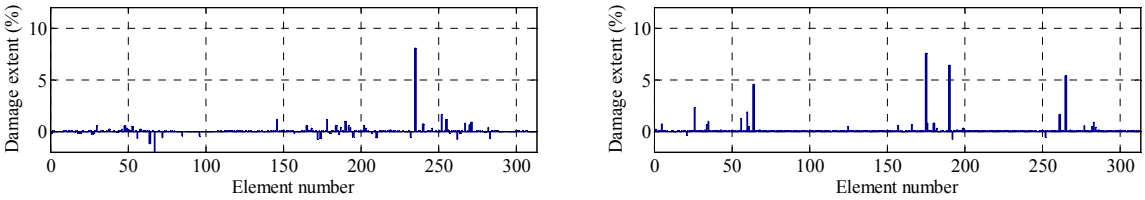

(a) (b)

Fig. 6. Damage identification results with 24 test points for three damage cases with 10% noise; (a) identification results of damage case 1 with 10% noise; (b) identification results of damage case 2 with 10% noise

5 Conclusions

A structural damage detection approach by combing CS theory and substructure sensitivity is proposed in the paper. The approach established the relationship between the substructure damage extent and the measured frequency vibration varying. Because the limitation of measurement degree of freedom of structure and incompletion of modal parameters, the established linear algebraic equation is ill-conditional. Based on the sparse phenomena of structure damage, i.e., the damage extent vector to be solved is sparse, the exact solutions can be obtained by CS theory. Numerical example of the 20-bay truss structure is carried out to valid the damage identification ability of the proposed approach with considering measurement noise. The proposed approach can identify multi-damages of structure including damage locations and extents with a small number of sensors, incomplete modal parameters and measurement noise. The sensor number will affect the damage identification accuracy, with the increasing of sensor number, the damage identification accuracy is increased and this effect is more significant to the multiple damage cases. Random placement of sensors is required in the approach, which has remarkable advantages in actual application of SHM systems. If one or small number of sensors are failed, the robust of damage identification results also can be obtained.

Acknowledgement

This research is supported by NSFC (Grant No. 51008095), and Ministry of Science and Technology (Grant No. 2011BAK02B02), and China Postdoctoral Science Special Foundation (Grant No. 201104439).

References

[1] Sohn H., Farrar C.R., Hemez F.M., Shunk D.D., Stinemates D.W., Nadler B.R., A Review of Structural Health Monitoring Literature: 1996-2001, LANL Report, LA-13976-MS, 2003.
[2] Yen, G.G., Lin and K.C. (2000), "Wavelet packet feature extraction for vibration monitoring", *IEEE T. Ind. Electron.*, 47(3), 650-667.
[3] J.N. Yang, Y. Lei, S. Lin, N. Huang. Hilbert-Huang Based Approach for Structural Damage Detection. ASCE Journal of Engineering Mechanics. 2004: 85-95.
[4] Vanik, M.W., Beck, J.L. and Au, S.K. (2000), "Bayesian probabilistic approach to structural health monitoring", *J. Eng. Mech.*, *ASCE*, 126(7), 738-745
[5] Candès EJ. Compressive Sampling. Proceedings of the International Congress of Mathematicians, Madrid, Spain; 2006, pp. 1433-52.
[6] Donoho D. Compressed Sensing. IEEE Trans Inform Theory 2006; 52(4): 1289-306.
[7] Baraniuk RG. Compressive sensing. IEEE Signal Process Mag 2007; 24(4), 118-21.
[8] Baraniuk RG. More is less: Signal processing and the data deluge. Science 2011; 331: 717-19.
[9] Zhao J., DeWolf J.T., Sensitivity study for vibrational parameters used in damage detection, Journal of Structural Engineering, 125(4), 1999.
[10] Boyd SP, Vandenberghe L. Convex Optimization, Cambridge Univ. Press, Cambridge, U K; 2004.
[11] Yao H, Gerstoft P, Shearer PM. Mecklenbrauker C. Compressive sensing of the Tohoku-Oki Mw 9.0 earthquake: Frequency-dependent rupture modes, Geophys Res Lett 2011; 38, L20310
[12] Malioutov DM, Müjdat C, Willsky AS. A sparse signal reconstruction perspective for source localization with sensor arrays. IEEE Trans Signal Process 2005; 53, 3010-3021.